

High Bandwidth Semi-Polar InGaN/GaN Micro-LEDs With Low Current Injection for Visible Light Communication

Feifan Xu¹, Pengjiang Qiu, Tao Tao¹, Pengfei Tian¹, Xiaoyan Liu¹, Ting Zhi, Zili Xie, Bin Liu¹, *Senior Member, IEEE*, and Rong Zhang

Abstract—Micro-light-emitting diodes (micro-LEDs) with high modulation rates and low power consumption could attract growing attention as visible light communication (VLC) technology advances. The designed and fabricated semi-polar micro-LEDs have achieved high bandwidth at low current injection due to the reduced quantum-confined Stark effect (QCSE), which was significantly greater than that of typical c-plane at the same current injection. Semi-polar green micro-LEDs got a -3 dB bandwidth that surpasses 500 MHz and 1 GHz at low current densities of 43.8 A/cm² and 120.6 A/cm², while blue micro-LEDs exceed 500 MHz at low current densities of 76.6 A/cm², respectively. Additionally, the free space VLC system has shown semi-polar blue and green micro-LED transmission data rates of 3.495 Gbps (433 A/cm²) and 3.483 Gbps (402 A/cm²) respectively. Semi-polar micro-LEDs, which can achieve low power consumption and high bandwidth, are anticipated to play a significant role in the development of energy-efficient VLC in the future.

Index Terms—Light-emitting diodes (LEDs), modulation bandwidth, semi-polar InGaN/GaN MQWs, visible light communication (VLC).

I. INTRODUCTION

IN RECENT years, visible light communication (VLC) technology has recently been regarded as one of the most important wireless data transfer techniques due to abundance of unlicensed spectrum resources, excellent security, and anonymity

Manuscript received 21 November 2022; revised 26 December 2022; accepted 5 January 2023. Date of publication 11 January 2023; date of current version 2 February 2023. This work was supported in part by the National Key R&D Program of China under Grants 2021YFB3601000 and 2021YFB3601002, in part by the National Nature Science Foundation of China under Grants 61974062, 62074077, 62004104, 61921005, and 61974031, in part by the Leading-edge Technology Program of Jiangsu Natural Science Foundation under Grant BE2021008-2, and in part by The Science Foundation of Jiangsu Province under Grants BK20202005 and BK20180747. (*Corresponding authors: Tao Tao; Pengfei Tian; Xiaoyan Liu; Bin Liu.*)

Feifan Xu, Tao Tao, Zili Xie, and Bin Liu are with the Jiangsu Provincial Key Laboratory of Advanced Photonic and Electronic Materials, School of Electronic Science and Engineering, Nanjing University, Nanjing 210093, China (e-mail: 15556926686@163.com; ttao@nju.edu.cn; xzl@nju.edu.cn; bliu@nju.edu.cn).

Pengjiang Qiu and Pengfei Tian are with the School of Information Science and Technology, Fudan University, Shanghai 200433, China (e-mail: 19210720058@fudan.edu.cn; pftian@fudan.edu.cn).

Xiaoyan Liu and Ting Zhi are with the College of Microelectronics, Nanjing University of Posts and Telecommunications, Nanjing 210093, China (e-mail: xiaoyanliu@njupt.edu.cn; zhit@njupt.edu.cn).

Rong Zhang is with the Jiangsu Provincial Key Laboratory of Advanced Photonic and Electronic Materials, School of Electronic Science and Engineering, Nanjing University, Nanjing 210093, China, and also with the Xiamen University, Xiamen 361005, China (e-mail: rzhang@nju.edu.cn).

Digital Object Identifier 10.1109/JPHOT.2023.3235108

[1], [2], [3], [4], [5]. High transfer speed light sources are fundamental for the VLC framework. The extraordinary advancements in GaN-based solid-state lighting (SSL) in ongoing 10 years have changed the VLC framework into accessible applications [6], [7], [8], [9]. A growing amount of importance will be given to LED light sources with high modulation rates and low power consumption as Internet of Things (IoT) technology advances. Conventional GaN micro-LEDs based on c-plane sapphire often require high operating current density to weaken the polarization field to obtain high bandwidth, but needing high power consumption. The quantum-confined Stark effect (QCSE), which is caused by the polarization field, limits the recombination lifetime of traditional c-plane LEDs to many dozens of nanoseconds [7], [10], [11]. Semi-polar and non-polar LED devices have strengthened the overlap of electron and hole wave functions in comparison to c-plane InGaN/GaN LED devices developed on sapphire substrates, which optimizes the radiation recombination efficiency [12], [13], [14]. These semi-polar or non-polar LED devices have displayed exceptional properties in comparison to traditional c-plane LEDs, including lower efficiency droop, a shorter carrier lifetime, and improved wavelength stability [14], [15], [16], [17]. The GaN-based semi-polar or non-polar LEDs are therefore thought to be a potential remedy to increase the transmission bandwidth at low current density [18], [19], [20]. Non-polar micro-LEDs have achieved a high bandwidth of 1.5 GHz at 1 kA/cm² and 1.0 GHz at a lower current density of 100 A/cm² [21], and a high bandwidth of 508 MHz at a low current density of 10 A/cm² has been demonstrated [22]. And micro-LEDs based on semi-polar structures with a -3 dB bandwidth of 756 MHz under a current density of 2.0 kA/cm² [18] and over 800 MHz for a relatively low current density of 385 A/cm² [15] have been demonstrated. The bandwidth of semi-polar micro-LEDs is inferior to non-polar at a low current density.

In this work, semi-polar (20-21) blue and green micro-LED devices were fabricated and investigated. The luminescence characteristics of semi-polar micro-LEDs were characterized by electroluminescence (EL) tests. After that, we characterized the frequency response characteristics of the semi-polar blue and green micro-LED and compared them with the c-plane micro-LED. The fabricated semi-polar micro-LEDs had a high bandwidth at low current injection, which was significantly greater than that of a typical c-plane at the same current injection.

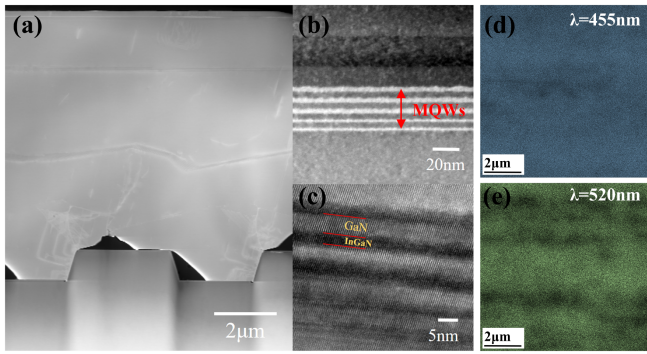


Fig. 1. (a) (b) (c) TEM and HRTEM images of the semi-polar (20–21) LEDs; (d) (e) CL mapping images probed at the wavelengths of 455 nm and 520 nm.

Additionally, the VLC system with optimized frequency division multiplexing (OFDM) modulation has been used to confirm the data transmission properties of these semi-polar micro-LEDs.

II. MATERIALS AND DEVICE FABRICATION

The epitaxial structure for manufacturing the semi-polar micro-LEDs was mainly composed of 6 μm thick Ge-doped GaN, 4 μm thick undoped GaN, 2 μm Si-doped n-type GaN layer, a 5 period InGaN/GaN multi-quantum wells (MQWs) with the emitting wavelength of 455 nm and 520 nm, and a 150 nm Mg-doped p-type GaN layer. A cross-sectional transmission electron microscope (TEM) and high-resolution transmission electron microscope (HRTEM) images of the semi-polar (20–21) LED epitaxial structure were shown in Fig. 1(a), (b), and (c). To filter and reduce the dislocations, two thinner quantum wells are grown initially, and three layers of quantum wells with a thickness of 4 nm were grown followed for the sake of acquiring higher In incorporation. It is suggested that the blurred interface is probably related to the step-like morphology of the GaN below, which is generally found in semi-polar GaN quantum wells grown on patterned substrates [13]. To investigate the distribution and formation of defects, the cathode luminescence mapping (CL-mapping) images were captured at different wavelengths corresponding to the blue LED wafer (455 nm) and green LED wafer (520 nm), as shown in Fig. 1(b). It can be seen that the areas with weaker green light emitting are relatively larger than that of the blue and show a streak-like distribution, that is widely observed in the surfaces of semi-polar and non-polar LED samples, caused by anisotropic growth rates in the growth plane [13]. Semi-polar GaN layers grown on foreign patterned substrates suffer from structural defects such as high densities of basal stacking faults (BSFs) and threading dislocations (TDs) [10], [23], [24], [25]. Efforts have been made on defect reduction and structure optimization to improve the semi-polar LED device's performance. In our previous reports, they have presented efficient semi-polar (20–21) InGaN/GaN multiple quantum wells grown on patterned sapphire substrate with internal quantum efficiency up to 52% [10]. Although there is still a large efficiency gap compared to the c-plane, the optimized semi-polar quantum well structure is a significant improvement over the efficiency of earlier semi-polar LEDs.

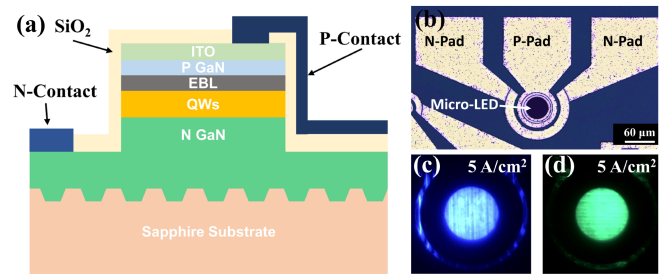


Fig. 2. (a) Schematic diagram of the semi-polar device; (b) Microscope image of the semi-polar micro-LED with the diameter of 60 μm ; (c) (d) EL images of blue and green emitting at a current density of 5 A/cm^2 .

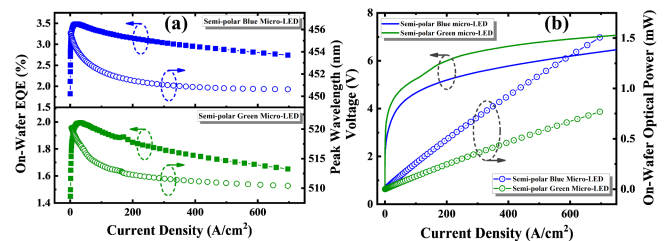


Fig. 3. (a) The variation curves of on-wafer EQE and luminescence peak with the injected current of semi-polar blue and green micro-LED. (b) The variation curves of voltage and on-wafer optical power with the injected current of semi-polar blue and green micro-LED.

The fabrication of micro-LED communication chips started with the growth of a 100 nm thick indium tin oxide (ITO) layer. A rapid thermal process (@600 $^{\circ}\text{C}/5\text{min}$) in an air atmosphere can effectively reduce the contact resistance with p-GaN. Mesa area with a diameter of 60 μm was defined by photolithography, the next etching depth was carefully controlled to be 1 μm by inductively coupled plasma (ICP) etching techniques. Subsequently, a 600 nm thick SiO_2 passivation layer was deposited by plasma-enhanced chemical vapor deposition (PECVD) for electrical isolation, and Ti/Al/Ti/Au with a thickness of 30/150/50/100 nm was deposited by electron beam evaporation (EBE) as the n/p electrodes, the structure schematic diagram of the micro-LEDs chip can be seen in Fig. 2(a) and the microscope image of the completed device is shown in Fig. 2(b). Fig. 2(c) and (d) show the EL image at a current density of 5 A/cm^2 .

III. RESULTS AND DISCUSSION

The forward luminescence of the micro-LED on the wafer was collected by the integrating sphere to obtain the absolute radiation spectrum, and the calculated EQE, emitting peak shift, and optical power are shown in Fig. 3. Comparable EQE curves were observed in semi-polar blue and green micro-LED, and the peak EQE of blue and green micro-LED is 3.49% and 1.99%. We can also observe an obvious shift in the peak EQE position concerning the emitting wavelength. In these terms, the EQE peak has shifted from 17.5 A/cm^2 of blue emitting to 32.3 A/cm^2 of green. This indicates that the semi-polar green InGaN/GaN MQWs have more non-radiative recombination centers compared to that of the blue LED. As the injected current density increases to $\sim 700 \text{ A}/\text{cm}^2$, the semi-polar blue

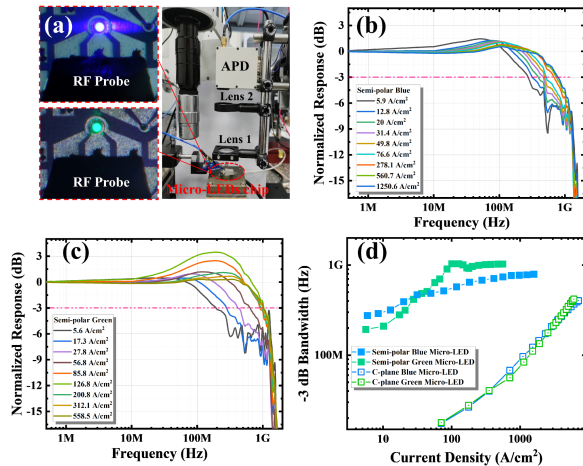


Fig. 4. (a) Realistic diagram for the frequency response measurement system. (b) (c) Results for the frequency response measurement of semi-polar blue and green micro-LED. (d) -3 dB bandwidth of semi-polar blue and green, c-plane blue and green micro-LED as a function of the current density.

micro-LED luminescence peak was shifted from 455.5 nm to 450.6 nm and the green was shifted from 520.2 nm to 510.4 nm, smaller than that of c-plane micro-LED thanks to the reduced QCSE [18], [26]. The current versus voltage (I-V) and on-wafer optical power-current (P-I) curve of semi-polar blue and green micro-LED can be found in Fig. 3(b). With the injected current density increasing to ~ 700 A/cm², the on-wafer optical power is over 1.51 mW and 0.73 mW corresponding to semi-polar blue and green light. The linear P-I characteristic can give a larger dynamic range to the visible light communication system, leaving a large room for the modulation signal changes and a higher signal-to-noise ratio (SNR).

Fig. 4(a) illustrates the test system for measuring the frequency response characteristics of the semi-polar micro-LED devices. The AC signals generated from the network analyzer were mixed with the DC drive by the bias-tee and were loaded onto the micro-LED through the RF probe (GSG-200, CASCADE). The light emitted from the micro-LED chip was collected by Lens 1 and focused by Lens 2, an avalanche photodiode (1.0 GHz, C5658, Hamamatsu,) has been used to capture the optical signal and converts it into an electrical signal and transmit it to the vector network analyzer (GA3623, ATTEN). The -3 dB bandwidth of semi-polar green micro-LED exceeds 500 MHz and 1 GHz at low current densities of 43.8 A/cm² and 120.6 A/cm², and achieves 1.035 GHz at a current density of 146 A/cm². The maximum bandwidth was limited by the frequency response of the APD. The -3 dB bandwidth of semi-polar blue micro-LED is over 300 MHz and 500 MHz at low current densities of 12.8 A/cm² and 76.6 A/cm² and reaches 790 MHz at 1584.7 A/cm². The corresponding -3 dB modulation bandwidth concerning injection current density was shown in Fig. 4(d). Conventional GaN micro-LEDs based on c-plane sapphire often require high operating current density to weaken the polarization field to obtain high bandwidth, but with high power consumption. Due to the increased overlap of electron-hole wave functions that accelerate carrier recombination, semi-polar blue and green micro-LED have achieved high

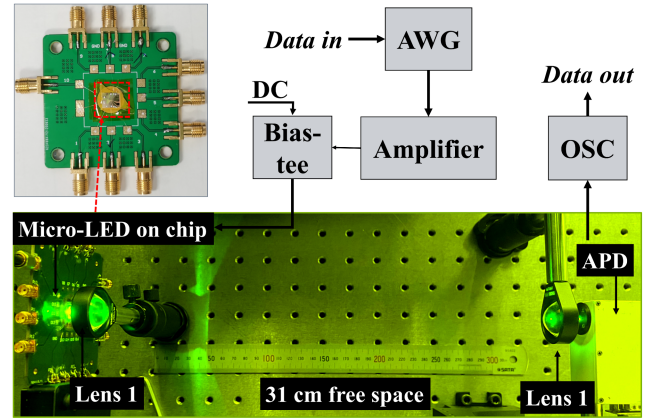


Fig. 5. The communication links of semi-polar green micro-LED VLC system.

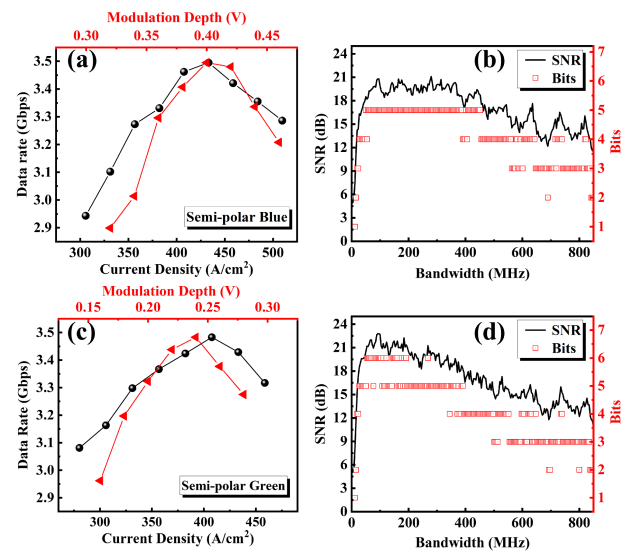


Fig. 6. (a) (c) The data rate versus injection current and modulation depth (V_{pp}) of semi-polar blue and green micro-LED; (b) (d) The SNR and bit-loading versus OFDM signal bandwidth of semi-polar blue and green micro-LED.

bandwidth at low current injection (less than 100 A/cm²), which is significantly greater than that of c-plane micro-LED at the same current injection, as shown in Fig. 4(d).

Fig. 5 shows the experimental results of the VLC system using optimized OFDM modulation to verify the data transmission characteristics of this semi-polar micro-LED. The micro-LED chip was fixed to the printed circuit board (PCB) and the modulation signal was input via an SMA connector. The compiled OFDM signals were uploaded to the arbitrary waveform generator (AWG710B, Tektronix) and loaded onto the micro-LED via a bias-tee and then an avalanche photodiode (C5658, Hamamatsu,) was used to capture the signals from the micro-LED light source with the distance of 0.31m and transmits it to the oscilloscope (DSA90604A, Agilent).

The optimal operating conditions of the semi-polar blue and green micro-LED-based VLC system were tested. Under different injected currents and modulation depths (V_{pp}), the data rates of the micro-LEDs VLC system with 850 MHz OFDM signals were tested and shown in Fig. 6(a) and (c). All curves

demonstrate a shape of ridge, the highest data rate of 3.495 Gbps and 3.483 Gbps for semi-polar blue and green micro-LED were achieved with a bit error rate (BER) of 2.03×10^{-3} and 2.62×10^{-3} , the injection current density of 433 A/cm² and 402 A/cm², and the V_{pp} of 0.4 V and 0.24 V, respectively. As shown in Fig. 6(b) and (d), the average SNRs are about 16.97 dB and 16.99 dB for semi-polar blue and green micro-LED within 850 MHz OFDM signals, respectively. It was sufficient for high-speed data transmission, and a high bit loading level of 5 corresponding to 32-QAM for semi-polar blue micro-LED and 6 corresponding to 64-QAM for green has been applied. It was shown that the transmitter based on semi-polar micro-LED can meet high-speed VLC. It can be seen the injection current corresponding to the maximum data rate is different from the injection current corresponding to the maximum - 3 dB bandwidth, because the data rate is determined by the bandwidth and SNR (relative to received optical power and distance).

IV. CONCLUSION

In summary, semi-polar blue and green micro-LEDs devices with a diameter of 60 μm exhibit high bandwidth at low current densities and are promising for use in energy-efficient VLC systems. The peak on-wafer EQE of the semi-polar blue and green devices are 3.49% and 1.99%, and the maximum on-wafer optical power can reach 1.51 mW and 0.73 mW at ~ 700 A/cm², respectively. The semi-polar InGaN/GaN structure has a significantly greater electron-hole wave function overlap, which allows the device to maintain a high bandwidth over GHz at low current densities. Moreover, a transmission data rate of 3.495 Gbps and 3.483 Gbps for semi-polar blue and green micro-LED has been demonstrated in a free space VLC system. To facilitate the rapid development of highly effective VLC applications, high-speed semi-polar micro-LEDs with low power are demanded.

REFERENCES

- [1] R. X. G. Ferreira et al., "High bandwidth GaN-based micro-LEDs for multi-Gb/s visible light communications," *IEEE Photon. Technol. Lett.*, vol. 28, no. 19, pp. 2023–2026, Oct. 2016, doi: [10.1109/lpt.2016.2581318](https://doi.org/10.1109/lpt.2016.2581318).
- [2] X. Liu et al., "High-bandwidth InGaN self-powered detector arrays toward MIMO visible light communication based on micro-LED arrays," *ACS Photon.*, vol. 6, no. 12, pp. 3186–3195, 2019, doi: [10.1021/acsp Photonics.9b00799](https://doi.org/10.1021/acsp Photonics.9b00799).
- [3] Z. Wei et al., "8.75 Gbps visible light communication link using an artificial neural network equalizer and a single-pixel blue micro-LED," *Opt. Lett.*, vol. 46, no. 18, pp. 4670–4673, Sep. 2021, doi: [10.1364/ol.437632](https://doi.org/10.1364/ol.437632).
- [4] O. Alkhazragi et al., "7.4-Gbit/s visible-light communication utilizing wavelength-selective semipolar micro-photodetector," *IEEE Photon. Technol. Lett.*, vol. 32, no. 13, pp. 767–770, Jul. 2020, doi: [10.1109/lpt.2020.2995110](https://doi.org/10.1109/lpt.2020.2995110).
- [5] F. F. Xu et al., "C-plane blue micro-LED with 1.53 GHz bandwidth for high-speed visible light communication," *IEEE Electron Device Lett.*, vol. 43, no. 6, pp. 910–913, Jun. 2022, doi: [10.1109/led.2022.3168314](https://doi.org/10.1109/led.2022.3168314).
- [6] Z. L. Chen et al., "High-brightness blue light-emitting diodes enabled by a directly grown graphene buffer layer," *Adv. Mater.*, vol. 30, no. 30, Jul. 2018, Art. no. 1801608. [Online]. Available: <http://WOS:000439737700021>
- [7] H. M. Huang, C. Y. Chang, Y. S. Hsu, T. C. Lu, Y. P. Lan, and W. C. Lai, "Enhanced internal quantum efficiency in graphene/InGaN multiple-quantum-well hybrid structures," *Appl. Phys. Lett.*, vol. 101, no. 6, Aug. 2012, Art. no. 061905. [Online]. Available: <http://WOS:000307862400017>
- [8] C. H. Kang et al., "Semipolar (20 $\bar{2}$) InGaN/GaN micro-photodetector for gigabit-per-second visible light communication," *Appl. Phys. Exp.*, vol. 13, 2020, Art. no. 014001, doi: [10.7567/1882-0786/ab58eb](https://doi.org/10.7567/1882-0786/ab58eb).
- [9] Y. Huang, Z. Guo, X. Wang, H. Li, and D. Xiang, "GaN-based high-response frequency and high-optical power matrix micro-LED for visible light communication," *IEEE Electron Device Lett.*, vol. 41, no. 10, pp. 1536–1539, Oct. 2020, doi: [10.1109/led.2020.3021282](https://doi.org/10.1109/led.2020.3021282).
- [10] M. Gong et al., "Semi-polar (20–21) InGaN/GaN multiple quantum wells grown on patterned sapphire substrate with internal quantum efficiency up to 52 per cent," *Appl. Phys. Exp.*, vol. 13, no. 9, 2020, Art. no. 091002, doi: [10.35848/1882-0786/abac91](https://doi.org/10.35848/1882-0786/abac91).
- [11] C. -C. Pan et al., "High-power, low-efficiency-droop semipolar (20 $\bar{2}$) single-quantum-well blue light-emitting diodes," *Appl. Phys. Exp.*, vol. 5, no. 6, 2012, Art. no. 062103, doi: [10.1143/apex.5.062103](https://doi.org/10.1143/apex.5.062103).
- [12] M. Monavarian et al., "Trade-off between bandwidth and efficiency in semipolar (20 $\bar{2}$) InGaN/GaN single- and multiple-quantum-well light-emitting diodes," *Appl. Phys. Lett.*, vol. 112, no. 19, 2018, Art. no. 191102, doi: [10.1063/1.5032115](https://doi.org/10.1063/1.5032115).
- [13] Y. Zhang et al., "Microstructure investigation of semi-polar (11-22) GaN overgrown on differently designed micro-rod array templates," *Appl. Phys. Lett.*, vol. 109, no. 24, Dec. 2016, Art. no. 241906, doi: [10.1063/1.4972403](https://doi.org/10.1063/1.4972403).
- [14] D. V. Dinh, Z. Quan, B. Roycroft, P. J. Parbrook, and B. Corbett, "GHz bandwidth semipolar (11 $\bar{2}$) InGaN/GaN light-emitting diodes," *Opt. Lett.*, vol. 41, no. 24, pp. 5752–5755, Dec. 2016, doi: [10.1364/OL.41.005752](https://doi.org/10.1364/OL.41.005752).
- [15] M. Haemmer et al., "Size-dependent bandwidth of semipolar (11 $\bar{2}$) light-emitting-diodes," *IEEE Photon. Technol. Lett.*, vol. 30, no. 5, pp. 439–442, Mar. 2018, doi: [10.1109/lpt.2018.2794444](https://doi.org/10.1109/lpt.2018.2794444).
- [16] J. I. Hagggar, Y. Cai, S. S. Ghataora, R. M. Smith, J. Bai, and T. Wang, "High modulation bandwidth of semipolar (11–22) InGaN/GaN LEDs with long wavelength emission," *ACS Appl. Electron. Mater.*, vol. 2, no. 8, pp. 2363–2368, Aug. 2020, doi: [10.1021/acsaem.0c00399](https://doi.org/10.1021/acsaem.0c00399).
- [17] M. Monavarian et al., "Explanation of low efficiency droop in semipolar (20 $\bar{2}$) InGaN/GaN LEDs through evaluation of carrier recombination coefficients," *Opt. Exp.*, vol. 25, no. 16, pp. 19343–19353, Aug. 2017, doi: [10.1364/OE.25.019343](https://doi.org/10.1364/OE.25.019343).
- [18] S. -W. H. Chen et al., "High-bandwidth green semipolar (20–21) InGaN/GaN micro light-emitting diodes for visible light communication," *ACS Photon.*, vol. 7, no. 8, pp. 2228–2235, 2020, doi: [10.1021/acsp Photonics.0c00764](https://doi.org/10.1021/acsp Photonics.0c00764).
- [19] Y. -H. Chang et al., "4.343-Gbit/s green semipolar (20-21) μ -LED for high speed visible light communication," *IEEE Photon. J.*, vol. 13, no. 4, Aug. 2021, Art. no. 7300204, doi: [10.1109/jphot.2021.3092878](https://doi.org/10.1109/jphot.2021.3092878).
- [20] C. Yun -Han et al., "High-speed white light visible light communication (VLC) based on semipolar (20-21) blue micro-light emitting diode (μ -LED)," in *Proc. Opt. Fiber Commun. Conf. Exhib.*, 2022, pp. 1–3.
- [21] A. Rashidi, M. Monavarian, A. Aragon, A. Rishinaramangalam, and D. Feezell, "Nonpolar m -plane InGaN/GaN micro-scale light-emitting diode with 1.5 GHz modulation bandwidth," *IEEE Electron Device Lett.*, vol. 39, no. 4, pp. 520–523, Apr. 2018, doi: [10.1109/led.2018.2803082](https://doi.org/10.1109/led.2018.2803082).
- [22] S. J. Zhu et al., "Low-power high-bandwidth non-polar InGaN micro-LEDs at low current densities for energy-efficient visible light communication," *IEEE Photon. J.*, vol. 14, no. 5, Oct. 2022, Art. no. 7351805, doi: [10.1109/jphot.2022.3204711](https://doi.org/10.1109/jphot.2022.3204711).
- [23] M. Khoury et al., "Polarized monolithic white semipolar (20–21) InGaN light-emitting diodes grown on high quality (20–21) GaN/sapphire templates and its application to visible light communication," *Nano Energy*, vol. 67, 2020, Art. no. 104236, doi: [10.1016/j.nanoen.2019.104236](https://doi.org/10.1016/j.nanoen.2019.104236).
- [24] S. Marcinkevicius, R. Ivanov, Y. Zhao, S. Nakamura, S. P. DenBaars, and J. S. Speck, "Highly polarized photoluminescence and its dynamics in semipolar (20 $\bar{2}$) InGaN/GaN quantum well," *Appl. Phys. Lett.*, vol. 104, no. 11, Mar. 2014, Art. no. 111113, doi: [10.1063/1.4869459](https://doi.org/10.1063/1.4869459).
- [25] H. Song, J. Suh, E. K. Kim, K. H. Baik, and S. -M. Hwang, "Growth of high quality a-plane GaN epi-layer on r-plane sapphire substrates with optimization of multi-buffer layer," *J. Cryst. Growth*, vol. 312, no. 21, pp. 3122–3126, Oct. 2010, doi: [10.1016/j.jcrysgro.2010.08.004](https://doi.org/10.1016/j.jcrysgro.2010.08.004).
- [26] F. F. Xu et al., "High-performance semi-polar InGaN/GaN green micro light-emitting diodes," *IEEE Photon. J.*, vol. 12, no. 1, Feb. 2020, Art. no. 2500107, doi: [10.1109/Jphot.2019.2962184](https://doi.org/10.1109/Jphot.2019.2962184).